Hippocampal Subregions Volume and Texture for the Diagnosis of Mild Cognitive Impairment

Tongpeng Chu
Yantai Yuhuangding Hospital, Affiliated Hospital of Qingdao University
Yajun Liu
Imaging Department, Liaocheng Infectious Disease Hospital
Zhongsheng Zhang
Yantai Yuhuangding Hospital, Affiliated Hospital of Qingdao University
Gang Zhang
Yantai Yuhuangding Hospital, Affiliated Hospital of Qingdao University
Fanghui Dong
Yantai Yuhuangding Hospital, Affiliated Hospital of Qingdao University
Jianli Dong
Yantai Yuhuangding Hospital, Affiliated Hospital of Qingdao University
Shujuan Lin (sdlsj123@126.com)
Yantai Yuhuangding Hospital, Affiliated Hospital of Qingdao University

Research Article

Keywords: Hippocampal subregions, Volume, Texture, Mild Cognitive Impairment, Diagnosis

Posted Date: January 10th, 2023

DOI: https://doi.org/10.21203/rs.3.rs-2182063/v2

Abstract

Purpose: The aim of this study was to examine the diagnostic efficacy of hippocampal subregions volume and texture in differentiating amnestic mild cognitive impairment (MCI) from normal aging changes.

Materials and Methods: Ninety MCI subjects and eighty-eight well-matched healthy controls (HCs) were selected from the ADNI-1 or ADNI-2 Database.Twelve hippocampal subregions volume and texture features were extracted using Freesurfer and MaZda based on T1 weighted magnetic resonance images. Then, two-sample t-test and Least Absolute Shrinkage and Selection Operator (LASSO) regression were developed to select a subset of the original features. Finally, a support vector machine (SVM) was used to perform the classification task and the area under the curve (AUC), sensitivity, specificity, and accuracy were calculated to evaluate the diagnostic efficacy of the model.

Results: The volume features with high discriminative power were mainly located in the bilateral CA1 and bilateral CA4, while texture feature were gray-level non-uniformity, run length non-uniformity and fraction. Our model based on hippocampal subregions volume and texture features achieved better classification performance with an AUC of 0.90.

Conclusions: Based on hippocampal subregions volume and texture can be used to diagnose MCI. Moreover, we found that the features that contributed most to the model were mainly textural features, followed by volume. These results may guide future studies using structural scans to classify patients with MCI.

1 Introduction

The incidence of dementia is rapidly increasing worldwide (Gauthier et al., 2016). Its most common cause is Alzheimer's disease (AD). Therapeutic interventions are important for alleviating the symptoms and delaying the progression of AD, but diseasemodifying treatments are not successful for patients with advanced AD (Doody et al., 2014; Prince et al., 2013). Mild cognitive impairment (MCI), refers to the prodromal phase of AD but without significant disability in daily life (Farias, Mungas, Reed, Harvey, & DeCarli, 2009). Early detection of ad can be further achieved by identifying MCI (Meyer, Xu, Thornby, Chowdhury, & Quach, 2002).

Hippocampal atrophy is one of the most sensitive biological indicators of AD (Hata et al., 2019), and hippocampal volumetry is the most well-established structural biomarker of AD, especially for early diagnosis (Moon, Lee, & Choi, 2018). Moreover, instead of being a homogeneous structure, the hippocampus consists of several subregions with different histological characteristics (Moon et al., 2018; Mueller, Schuff, Raptentsetsang, Elman, & Weiner, 2008), each of which has been assigned a specific functions (Prasad et al., 2019). The association of hippocampal subregions abnormalities and cognitive impairment is well established in AD (La Joie et al., 2013), vascular dementia (Li et al., 2016), and other disorders associated with cognitive impairment (Prasad et al., 2019). Hippocampal subregions volume

have recently been recommended as more specific neuroimaging markers for AD compared to conventional global hippocampal or medial temporal lobe atrophy (Wong et al., 2021).

The combination of different neuroimaging measures may help to improve the diagnosis and prediction of AD, as single biomarkers only represent a specific stage of the ad process and their combination may provide complementary information (Gao et al., 2018). For example, it has been shown that the shape and texture of the hippocampus provide diagnostic information independent of hippocampal volume (Achterberg et al., 2014; Sorensen et al., 2016). The presence of abnormal hippocampal texture, alone or in combination with data from other modalities, has been shown to be a promising neuroimaging biomarker for the diagnosis and prediction of AD (Eskildsen et al., 2013; Sorensen et al., 2017).

Machine learning techniques are highly effective in processing high-dimensional data, among which support vector machines (SVM), the most widely studied data mining technique, have been widely used to develop diagnostic algorithms for various diseases, including AD diagnosis and prediction (Eskildsen et al., 2013; Jack et al., 2012; F. Zhang, Petersen, Johnson, Hall, & O'Bryant, 2021).

In summary, hippocampal volume or texture or hippocampal subregions volume received moderate to good classification in the diagnosis of MCI, but whether a combined biomarker combining hippocampal subregions volume and texture features would achieve better diagnostic performance is unknown. In this study, we will use an SVM algorithm to build a model to classify MCI patients and healthy controls (HCs) based on hippocampal subregions volume and texture features. The flowchart of this study is shown in Fig. 1.

2 Material And Methods

2.1 Participants

A total of 178 right-handed participants were selected from the ADNI-1 or ADNI-2 (https://adni.loni.usc.edu/) and enrolled in this study. The ADNI-1 cohort comprised 68 patients diagnosed with MCI (Clinical Dementia Rating ,CDR = 0.5)(Morris, 1993) and 68 HCs, while the ADNI-2 comprised 22 patients diagnosed with MCI (CDR = 0.5) and 20 HCs (Table 1). The clinical and demographic information about the subjects is provided in (Marcus et al., 2007).

Table 1
Demography of MCI and patients with HCs

ADNI-1	**MCI (n = 68)**	**HCs (n = 68)**	***P***
Age	76.51 ± 7.04	75.87 ± 8.74	0.58
Gender(F/M)	38/30	42/26	0.51
MMSE scores	25.56 ± 3.51	29.01 ± 1.23	< 0.001**
ADNI-2	**MCI (n = 22)**	**HCs (n = 20)**	P
Age	74.82 ± 8.75	77.15 ± 7.62	0.97
Gender(F/M)	11/11	12/8	0.36
MMSE scores	24.32 ± 4.20	27.60 ± 2.48	0.004*
Notes: Group differences between the MCI and HCs groups were analyzed by two-sample t test for age and MMSE or χ2 (chi-squared) test for gender. Values are expressed as the mean ± SD. MMSE: Mini-Mental State Examination (MMSE)			

2.2 Image Acquisition

All calculations in this study were performed using the first baseline scan. The images were acquired in the sagittal plane with a spoiled gradient recalled (SPGR) sequence for the anatomic images. Structural imaging was conducted using the following parameters: TR = 9.7ms, TE = 4.0ms, TI = 20ms, flip angle = 10°, sagittal orientation with 128 slices, and resolution = 1 × 1 × 1.25mm^3.

2.3 Image Preprocessing

All images were preprocessed with FreeSurfer. The images included motion correction and confirmation, nonuniform intensity standardization, Talairach transform calculation, intensity standardization, skull removal, and neck removal. The software can be downloaded online for public use (http://www.freesurfer.net/fswiki/DownloadAndInstall/). Quality control analysis of Freesurfer reconstruction included automatic detection of recon-all processing errors and visual inspection for segmentation, intensity normalization, and skull stripping errors(Jiang et al., 2015). One HCs of ADNI-1 was excluded for recon-all errors, and two MCI subjects of ADNI-2 were excluded for segmentation errors noted with visual inspection.

2.4 Image Segmentation and Feature Extraction

FreeSurfer automatically segments the hippocampal subregions on the basis of statistical maps constructed from ultra-high resolution (~ 0.1 mm isotropic) in vitro MRI data(Wisse et al., 2012). Recent studies have confirmed the reliability of FreeSurfer in segmenting the hippocampal subregions(Brown et al., 2020). The hippocampus was divided into 12 subregions, namely, parasubiculum, presubiculum, subiculum, CA1, CA3, CA4, GC-DG, HATA, fimbria, molecular_layer_HP, hippocampal_fissure, and HP_tail(Iglesias, 2015), no head/body subdivision for the hippocampal subregions. The way in which

labels are merged in the volume is summarized in http://surfer.nmr.mgh.harvard.edu/fswiki/HippocampalSubfieldsAndNucleiOfAmygdala. After this module was run, the volumes of all the subjects' hippocampal subregions were collected and written in a file.

MaZda (version 5.3.0) was used to calculate texture features, which can be downloaded for public use online (http://www.eletel.p.lodz.pl/programy/mazda/) (Szczypiński et al., 2009). According to our previous study (Yang et al., 2021), in MaZda, five various run-length matrices are computed for five pixel run directions: horizontal (Horzl_), vertical (Vertl_), slanted at 45 degrees (45dgr_), slanted at 135 degrees (135dgr_), and z. There are five run-length matrix-based features computed for each of the matrices: short run emphasis inverse moment, long run emphasis moment, gray-level non-uniformity, run length non-uniformity and fraction of image in runs(Haralick, 1979).

2.5 Feature Engineering

The hippocampal subregions volume and texture were defined as the features. The extracted features were standardized to remove the unit limit of each feature and reduced the computational complexity of the model. In this work, a two-stage feature selection procedure was developed to select a subset of the original features (Chen et al., 2017). Firstly, we adopted two-sample t-test to select features with statistically significant differences between MCI and HCs ($p < 0.05$). Secondly, Least Absolute Shrinkage and Selection Operator (LASSO) regression was used to further optimize the feature subset (Friedman, Hastie, & Tibshirani, 2010).

2.6 Classification and Model Evaluation

In this study, SVM was used to perform the classification task. All subject were divided as a training set and a test set by ten-fold cross validation. A five-fold cross-validation loop was implemented to determine the optimal hyper parameters and avoid data leakage (Patel, Khalaf, & Aizenstein, 2016). The test set is utilized to test and estimate the performance of the classifier with an optimal hyper-parameter model. The receiver operating characteristic (ROC) curve of the model was drawn, and the area under the curve (AUC), sensitivity, specificity, and accuracy were calculated to evaluate the diagnostic efficacy of the model.

2.7 Identification of features with high discriminative power

To understand the abnormal hippocampal subregions in MCI compared to HC, features with high discriminative power were identified. The discriminative power of a feature was according to its averaged weights in 10 experiments on the 10-fold cross-validation (Arbabshirani, Plis, Sui, & Calhoun, 2017).

2.8 Statistical Analysis

Feature engineering classification and model evaluation were implemented used a python module named easylearn (https://github.com/lichao312214129/easylearn). Easylearn is built on top of scikit-

learn (https://dl.acm.org/doi/10.5555/1953048.2078195), and designed for machine learning mainly in resting-state fMRI, radiomics and other fields (such as EEG).

The differences in the demographic data between HCs and patients with MCI were computed by the independent two sample t-test or χ2 (chi-squared) test with the IBM Statistical Package for the Social Sciences 24.0 software. The significance level was set to $p < 0.05$. Values are expressed as the mean ± SD.

3 Results

3.1 Demographic Data

The demographic and clinical data are described in Table 1. No significant differences in gender and age were found between the MCI group and the HCs. MMSE scores between groups were significantly different.

3.2 Feature Engineering

To further explore altered hippocampal subregions in MCI relative to HCs, we calculated the average weight of each selected feature across all cross validation paths. The volume features with high discriminative power were mainly located in the bilateral CA1, and bilateral CA4, while texture feature were gray-level non-uniformity, run length non-uniformity and fraction. Table 2 shows the top 10 most discriminative features and corresponding hippocampal regions.

Table 2
Top 10 most discriminative features and corresponding hippocampal subregions

Features		Region	|w|
Texture	gray-level non-uniformity	left CA1	15.773
	run length non-uniformity	right CA4	13.977
	gray-level non-uniformity	left CA4	12.214
	run length non-uniformity	right hippocampal tail	10.806
	gray-level non-uniformity	right CA1	8.892
	fraction	right HATA	7.516
Volume		right CA1	6.728
		left CA1	5.806
		left CA4	3.886
		right CA4	2.687

3.3 Classification and Model Evaluation

As shown in Fig. 2, our model based on hippocampal subregions volume and texture features achieved better classification performance with an AUC of 0.90. Table 3 shows the classification performance of previous studies, and the results suggest that hippocampal subregions volume and texture combination may improve the diagnostic performance of MCI.

Table 3
Performance Comparison of Different Methods in MCI/HCs Classification

	Method	Features	Accuracy	Sensitivity	Specificity	AUC
Luk, Collin C et al.	SVM	hippocampal texture	\	0.71	0.79	0.82
Gao, Ni et al.	Gaussian process	hippocampal texture, Clinical, volume-based morphometric parameters	79.50	\	\	\
	partial least squares		83.60	\	\	\
Sørensen, Lauge et al.	SVM	cortical thickness, hippocampal shape, hippocampal texture, volumetry	\	\	\	0.68
Sørensen, Lauge et al.	Logistic Regression	hippocampal volume	\	\	\	0.74
		hippocampal texture	\	\	\	0.70
		hippocampal texture, hippocampal volume	\	\	\	0.74
Feng, Feng et al.	SVM	radiomic features of hippocampal subregions	0.71	0.80	0.58	\
Proposed	SVM	hippocampal subregions volume and texture	0.84	0.88	0.78	0.90

4 Discussion

In this study, a combined biomarker combining hippocampal subregions volume and texture features could achieve better diagnostic performance. Showed that imaging measures assessing different subregions of the hippocampus provide more accurate and sensitive information for diagnosing patients with MCI. Further illustrate that different locations of the hippocampus differ in their sensitivity to neuropathology. Moreover, we found that the features that contributed most to the model were mainly textural features, followed by volume. Showed that texture features play an important role in image analysis studies and may develop into a useful clinical imaging tool. Texture analysis provides a

quantitative method to analyze and characterize tissue properties, physiological and pathological stages, and reveals information that is not normally visible on the tissue of interest (Nanni, Brahnam, Salvatore, Castiglioni, & Alzheimer's Disease Neuroimaging, 2019; J. Zhang, Yu, Jiang, Liu, & Tong, 2012)

The volume and texture features with high discriminative power were mainly located in the bilateral CA1, and bilateral CA4. Previous studies have shown that CA1, one of the three core synaptic stations of the “trisynaptic circuit” (Stepan, Dine, & Eder, 2015), were the most atrophic subfields in patients with verbal and visual memory impairment. In line with this, histopathological studies on AD disclosed CA1 decreased hippocampal neuronal density and dendritic abnormalities (Cacciaguerra et al., 2021; Padurariu, Ciobica, Mavroudis, Fotiou, & Baloyannis, 2012). The core pathological markers of AD are amyloid and neurofibrillary tangles (NFTs) (Huang et al., 2022). Neuropathological studies have shown that NFTs are transmitted along CA1 to CA4 along the AD continuum (Ciarmiello et al., 2019). In addition, the volume of CA4 was smaller in patients whose MCI converted AD than in those who did not convert to AD (Barry, Clark, & Maguire, 2021). Showed that calculating the features of hippocampal subregions, especially CA1 and CA4, had a higher sensitivity than the whole hippocampus in the differential diagnosis and prognosis of MCI.

However, several major limitations should be mentioned. First, in this study, the FreeSurfer software hippocampus automatic segmentation tool was used. Although recent studies have confirmed the reliability of FreeSurfer in segmenting hippocampal subregions (Brown et al., 2020), different anatomical templates and tools still inevitably produce errors. Subsequent studies may need to assess the differences and influence of various software and anatomical templates. Second, the present study is a cross-sectional study, and future research could use longitudinal data on altered values of volume and texture of hippocampal subregions. Finally, our study demonstrates that features of hippocampal subregions could improve the diagnostic performance of MCI, which should be extracted later in combination with multimodal data given the heterogeneity of MR imaging modalities.

5 Conclusions

Our results suggest that features of the combined volume and texture in the hippocampal subregions could be useful for the diagnosis of MCI. The features contributed most to model classification were mainly located in bilateral CA1, and bilateral CA4, while textural features contributed more weight values. These results may guide future studies using high-resolution structural scans and finer delineation of anatomic tissue to classify patients with MCI.

Declarations

Ethics approval and consent to participate

All participants signed an informed consent after a detailed description of the research, which was approved by the ADNI Executive Committee. Permissions for this study were obtained from the ADNI

database. Interested scientists may obtain access to ADNI imaging, clinical, genomic, and biomarker data for the purposes of scientific investigation, teaching, or planning clinical research studies. Access is contingent on adherence to the ADNI Data Use Agreement. The publications' policies are detailed in https://adni.loni.usc.edu/data-samples/access-data/.

The study was approved by the Research Ethics Committee of Yantai Yuhuangding Hospital. All methods were carried out in accordance with relevant guidelines and regulations.

Consent for publication

Not Applicable

Availability of data and materials

A total of 178 right-handed participants were selected from the ADNI-1 or ADNI-2 (https://adni.loni.usc.edu/)

Competing interests

The authors declare that they have no competing interests.

Funding

Not applicable.

Authors' contributions

Acquisition, analysis, or interpretation of data: TC, YL and ZZ. Drafting of the manuscript: TC and YL. Critical revision of the manuscript for important intellectual content: GZ, FD and SL. Statistical analysis: TC and FD. Technical, or material support: JD and SL.

Acknowledgements

Not applicable.

References

1. Achterberg HC, van der Lijn F, den Heijer T, Vernooij MW, Ikram MA, Niessen WJ, et al. Hippocampal shape is predictive for the development of dementia in a normal, elderly population. Hum Brain Mapp. 2014;35(5):2359–71.
2. Arbabshirani MR, Plis S, Sui J, Calhoun VD. Single subject prediction of brain disorders in neuroimaging: Promises and pitfalls. NeuroImage. 2017;145(Pt B):137–65.
3. Barry DN, Clark IA, Maguire EA. The relationship between hippocampal subfield volumes and autobiographical memory persistence. Hippocampus. 2021;31(4):362–74.

4. Brown EM, Pierce ME, Clark DC, Fischl BR, Iglesias JE, Milberg WP, et al. Test-retest reliability of FreeSurfer automated hippocampal subfield segmentation within and across scanners. NeuroImage. 2020;210:116563.
5. Cacciaguerra L, Valsasina P, Meani A, Riccitelli GC, Radaelli M, Rocca MA, et al. Volume of hippocampal subfields and cognitive deficits in neuromyelitis optica spectrum disorders. Eur J Neurol. 2021;28(12):4167–77.
6. Chen X, Zhang H, Zhang L, Shen C, Lee SW, Shen D. Extraction of dynamic functional connectivity from brain grey matter and white matter for MCI classification. Hum Brain Mapp. 2017;38(10):5019–34.
7. Ciarmiello A, Giovannini E, Riondato M, Giovacchini G, Duce V, Ferrando O, et al. Longitudinal cognitive decline in mild cognitive impairment subjects with early amyloid-β neocortical deposition. Eur J Nucl Med Mol Imaging. 2019;46(10):2090–8.
8. Doody RS, Thomas RG, Farlow M, Iwatsubo T, Vellas B, Joffe S, et al. Phase 3 trials of solanezumab for mild-to-moderate Alzheimer's disease. N Engl J Med. 2014;370(4):311–21.
9. Eskildsen SF, Coupé P, García-Lorenzo D, Fonov V, Pruessner JC, Collins DL. Prediction of Alzheimer's disease in subjects with mild cognitive impairment from the ADNI cohort using patterns of cortical thinning. NeuroImage. 2013;65:511–21.
10. Farias ST, Mungas D, Reed BR, Harvey D, DeCarli C. Progression of mild cognitive impairment to dementia in clinic- vs community-based cohorts. Arch Neurol. 2009;66(9):1151–7.
11. Friedman J, Hastie T, Tibshirani R. Regularization Paths for Generalized Linear Models via Coordinate Descent. J Stat Softw. 2010;33(1):1–22.
12. Gao N, Tao LX, Huang J, Zhang F, Li X, O'Sullivan F, et al. Contourlet-based hippocampal magnetic resonance imaging texture features for multivariant classification and prediction of Alzheimer's disease. Metab Brain Dis. 2018;33(6):1899–909.
13. Gauthier S, Feldman HH, Schneider LS, Wilcock GK, Frisoni GB, Hardlund JH, et al. Efficacy and safety of tau-aggregation inhibitor therapy in patients with mild or moderate Alzheimer's disease: a randomised, controlled, double-blind, parallel-arm, phase 3 trial. Lancet. 2016;388(10062):2873–84.
14. Hata K, Nakamoto K, Nunomura A, Sone D, Maikusa N, Ogawa M, et al. Automated Volumetry of Medial Temporal Lobe Subregions in Mild Cognitive Impairment and Alzheimer Disease. Alzheimer Dis Assoc Disord. 2019;33(3):206–11.
15. Huang Y, Huang L, Wang Y, Liu Y, Lo CZ, Guo Q. Differential associations of visual memory with hippocampal subfields in subjective cognitive decline and amnestic mild cognitive impairment. BMC Geriatr. 2022;22(1):153.
16. Iglesias JE, Augustinack JC, Nguyen K, Player CM, Player A, Wright M, Roy N, Frosch MP, Mc Kee AC, Wald LL, Fischl B, Van Leemput K. A computational atlas of the hippocampal formation using ex vivo, ultra-high resolution MRI: Application to adaptive segmentation of in vivo MRI. NeuroImage. 2015;115(1):117–37.

17. Jack CR Jr, Vemuri P, Wiste HJ, Weigand SD, Lesnick TG, Lowe V, et al. Shapes of the trajectories of 5 major biomarkers of Alzheimer disease. Arch Neurol. 2012;69(7):856–67.
18. Jiang Y, Guo X, Zhang J, Gao J, Wang X, Situ W, et al. Abnormalities of cortical structures in adolescent-onset conduct disorder. Psychol Med. 2015;45(16):3467–79.
19. La Joie R, Perrotin A, de La Sayette V, Egret S, Doeuvre L, Belliard S, et al. Hippocampal subfield volumetry in mild cognitive impairment, Alzheimer's disease and semantic dementia. Neuroimage Clin. 2013;3:155–62.
20. Li X, Li D, Li Q, Li Y, Li K, Li S, et al. Hippocampal subfield volumetry in patients with subcortical vascular mild cognitive impairment. Sci Rep. 2016;6:20873.
21. Marcus DS, Wang TH, Parker J, Csernansky JG, Morris JC, Buckner RL. Open Access Series of Imaging Studies (OASIS): Cross-sectional MRI Data in Young, Middle Aged, Nondemented, and Demented Older Adults. J Cogn Neurosci. 2007;19(9):1498–507.
22. Meyer JS, Xu G, Thornby J, Chowdhury MH, Quach M. Is mild cognitive impairment prodromal for vascular dementia like Alzheimer's disease? Stroke. 2002;33(8):1981–5.
23. Moon SW, Lee B, Choi YC. Changes in the Hippocampal Volume and Shape in Early-Onset Mild Cognitive Impairment. Psychiatry Investig. 2018;15(5):531–7.
24. Morris JC. The Clinical Dementia Rating (CDR): Current version and scoring rules. Neurology. 1993;43(11):2412–2.
25. Mueller SG, Schuff N, Raptentsetsang S, Elman J, Weiner MW. Selective effect of Apo e4 on CA3 and dentate in normal aging and Alzheimer's disease using high resolution MRI at 4 T. NeuroImage. 2008;42(1):42–8.
26. Nanni L, Brahnam S, Salvatore C, Castiglioni I, & Alzheimer's Disease Neuroimaging, I. (2019). Texture descriptors and voxels for the early diagnosis of Alzheimer's disease. *Artif Intell Med, 97*, 19–26.
27. Padurariu M, Ciobica A, Mavroudis I, Fotiou D, Baloyannis S. Hippocampal neuronal loss in the CA1 and CA3 areas of Alzheimer's disease patients. Psychiatr Danub. 2012;24(2):152–8.
28. Patel MJ, Khalaf A, Aizenstein HJ. Studying depression using imaging and machine learning methods. Neuroimage Clin. 2016;10:115–23.
29. Prasad S, Shah A, Bhalsing KS, Kumar KJ, Saini J, Ingalhalikar M, et al. Abnormal hippocampal subfields are associated with cognitive impairment in Essential Tremor. J Neural Transm (Vienna). 2019;126(5):597–606.
30. Prince M, Bryce R, Albanese E, Wimo A, Ribeiro W, Ferri CP. The global prevalence of dementia: a systematic review and metaanalysis. Alzheimers Dement. 2013;9(1):63–75.e62.
31. Sorensen L, Igel C, Liv Hansen N, Osler M, Lauritzen M, Rostrup E, et al. Early detection of Alzheimer's disease using MRI hippocampal texture. Hum Brain Mapp. 2016;37(3):1148–61.
32. Sorensen L, Igel C, Pai A, Balas I, Anker C, Lillholm M, et al. Differential diagnosis of mild cognitive impairment and Alzheimer's disease using structural MRI cortical thickness, hippocampal shape, hippocampal texture, and volumetry. Neuroimage Clin. 2017;13:470–82.

33. Stepan J, Dine J, Eder M. Functional optical probing of the hippocampal trisynaptic circuit in vitro: network dynamics, filter properties, and polysynaptic induction of CA1 LTP. Front Neurosci. 2015;9:160.
34. Wisse LEM, Gerritsen L, Zwanenburg JJM, Kuijf HJ, Luijten PR, Biessels GJ, et al. Subfields of the hippocampal formation at 7 T MRI: In vivo volumetric assessment. NeuroImage. 2012;61(4):1043–9.
35. Wong FCC, Yatawara C, Low A, Foo H, Wong BYX, Lim L, et al. Cerebral Small Vessel Disease Influences Hippocampal Subfield Atrophy in Mild Cognitive Impairment. Transl Stroke Res. 2021;12(2):284–92.
36. Yang C, Ren J, Li W, Lu M, Wu S, Chu T. Individual-level morphological hippocampal networks in patients with Alzheimer's disease. Brain Cogn. 2021;151:105748.
37. Zhang F, Petersen M, Johnson L, Hall J, O'Bryant SE. Recursive Support Vector Machine Biomarker Selection for Alzheimer's Disease. J Alzheimers Dis. 2021;79(4):1691–700.
38. Zhang J, Yu C, Jiang G, Liu W, Tong L. 3D texture analysis on MRI images of Alzheimer's disease. Brain Imaging Behav. 2012;6(1):61–9.

Figures

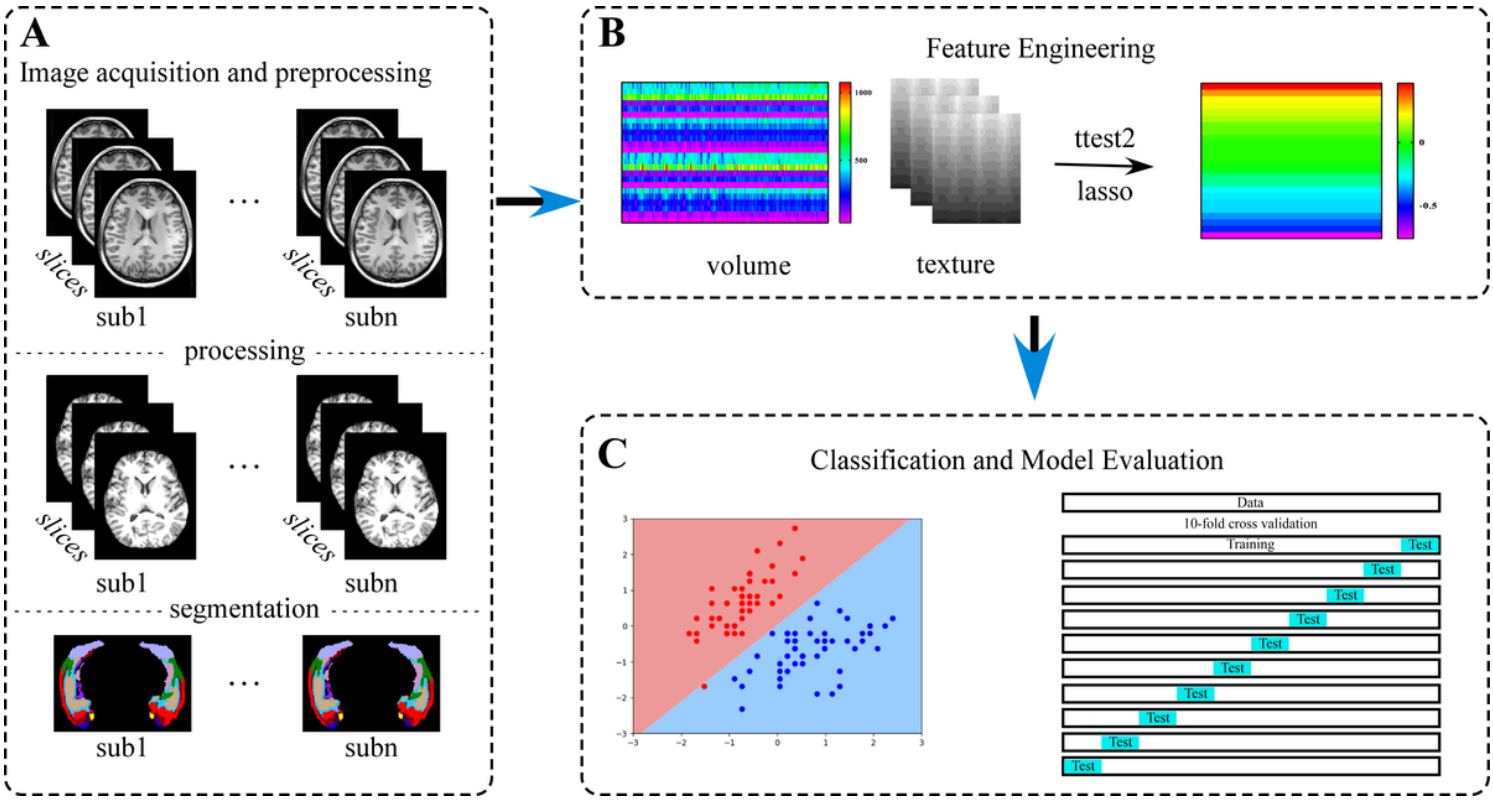

Figure 1

Workflow used in this study.

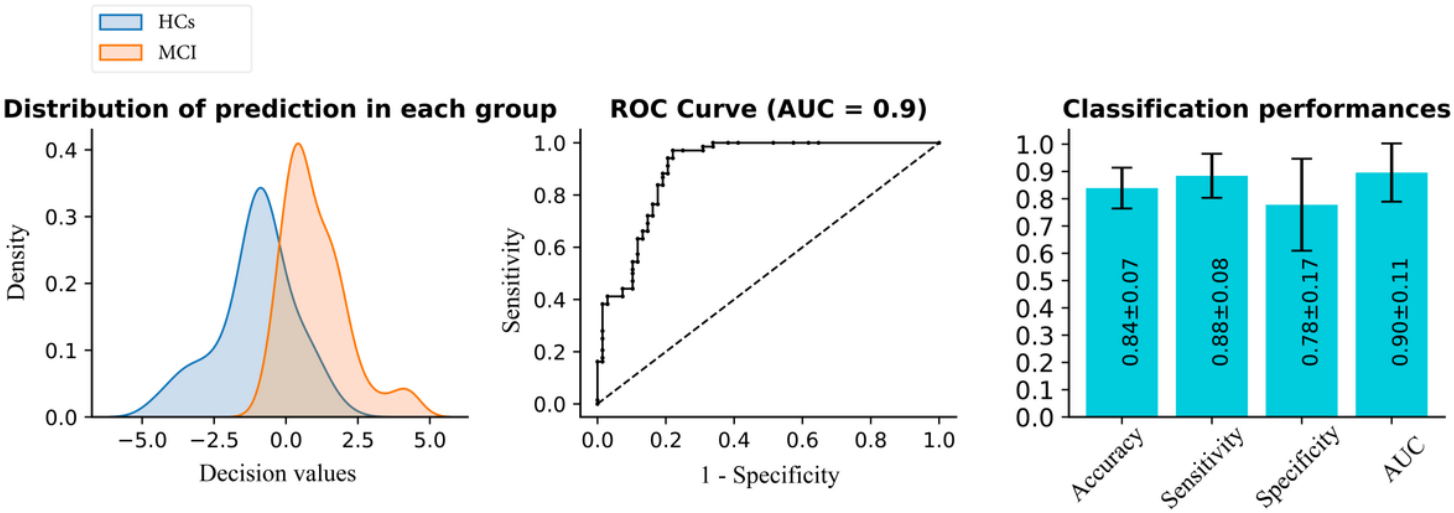

Figure 2

Classification performance of SVM model based on hippocampal subregions volume and texture features.